Highly Flexible and Ultra-Precise Manipulation of Light Levitated Femtolitre/Picolitre Droplets

Long Jiao [a,b], Rong Chen [a,b]*, Xun Zhu [a,b]*, Qiang Liao [a,b]*, Hong Wang [a,b], Liang An [c], Jie Zhu [c], Xuefeng He [a,b], Hao Feng [a,b]

[a] Key Laboratory of Low-grade Energy Utilization Technologies and Systems (Chongqing University), Ministry of Education, Chongqing 400030, China

[b] Institute of Engineering Thermophysics, School of Energy and Power Engineering, Chongqing University, Chongqing 400030, China

[c] Department of Mechanical Engineering, The Hong Kong Polytechnic University, Hong Kong, China

Corresponding authors

*Email: rchen@cqu.edu.cn (Rong Chen), *Email: zhuxun@cqu.edu.cn (Xun Zhu), *Email: lqzx@cqu.edu.cn (Qiang Liao)

Abstract

The ultra-precise manipulation of the droplets at the microscale is a promising paradigm for broad implications in reagent transport and element analysis but the existing strategies still suffer from the cross-contamination or the miscellaneous auxiliaries. Inspired by the levitation, we develop a method for excellently manipulating levitated femtolitre/picolitre droplets by a single focused laser. We show that the unique light-induced vapor flow in association with the interface morphology is responsible for creation and manipulation of levitated droplets. In particular, we demonstrate that the levitated droplets formed by this light method show extraordinary motility. The highly-accurate two-dimensional labyrinth movement of the levitated droplets with designed trajectories above the free surface is easily realized by scanning the light. These results

demonstrate that a single focused light can function as an ‘optical baton’ to enable us to construct a wide variety of the long-sought precise manipulation systems for bioassays, pharmacy and chemosynthesis.

TOC Graphic

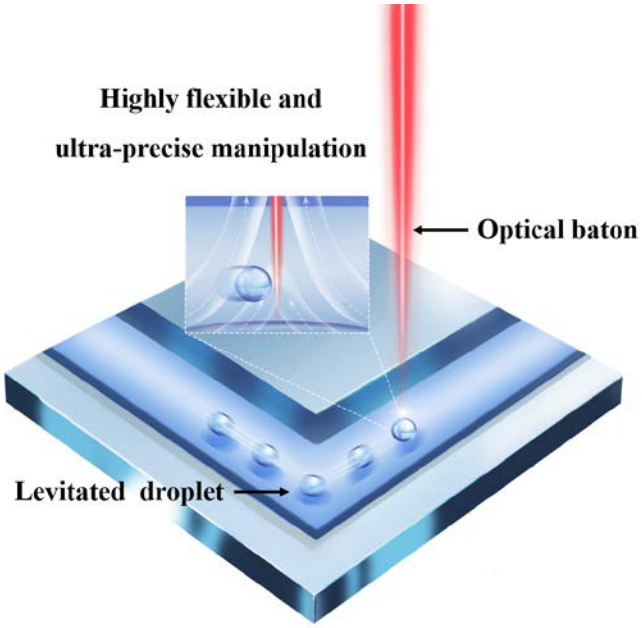

Manipulating small liquid droplets to perform reactions and analysis is crucial in microfluidics with great impacts on science due to its broad implications in bioassays, pharmacy, immunoassays and synthesis of nanomaterials [1-4]. Several techniques to trace and manipulate the droplets have been proposed. However, conventional droplet manipulation usually relies on complex architectures of digital lab-chip devices, micro-orifices and droplets splitting based on elaborate surface treatment technologies [5-8]. Using the conventional methods for the arduous manipulation of the small size droplets poses several grand challenges, such as cross-contamination of reagents, viscous resistance caused by the wetting and limited droplet motion precision, especially for the extremely small femtolitre/picolitre droplets. Hence, the improvement in flexibility and precision of the droplet-actuation at the microscale are highly desired, which is necessary for the great progress of these schemes [9-11].

Droplets levitation is possibly able to well address the above issues because of the unique properties of levitated objects, including the contactless state and the attrition-free. Right now, droplets levitation has been realized by several mechanisms, including magnetic levitation [12, 13], electrostatic levitation [14, 15], acoustic levitation [16-17]. However, existing methods usually require severe conditions (such as Earnshaw's theorem for paramagnetic levitation and electrostatic levitation, superconductor for diamagnetic levitation, acoustic pressure nodes for acoustic levitation and miscellaneous auxiliaries for acoustics-controlled motility) or restricted materials, leading to the imprecise and unhandy trace and motion of levitated objects and restricting their widespread applications [18-20]. One particularly promising research area emerges to allow for the highly flexible and precise manipulation of the levitated droplets by using a light as an external stimulus [21, 22]. Light is regarded as a particularly proper stimulus to actuate small liquid droplets

as it can provide distinct merits, including remote control, tunability of the intensity and prominent spatial and temporal resolution [23-28]. Notably, due to the well configurability of the light, various operations and multipath concurrency control can be performed with a light beam by using holographic techniques to generate the complex light patterns and the laser moving path can be easily adjusted and reset [29-31]. Therefore, the manipulation of the levitated femtolitre/picolitre droplets with complex and independent path by the light method become feasible. However, although the significant potentials of the existing light strategies have been demonstrated, few attention has been paid to the directional light-dominated transportability of the levitated droplets. While the flexible and accurate manipulation of the droplets is significantly important due to its crucial role in the corresponding applications of the materials transport and the follow-up biochemical reactions/analysis.

In this work, to break up these essential roadblocks, we develop a light method for optically manipulating femtolitre/picolitre droplets levitated above a free surface by the photothermal effect of a single focused light without the miscellaneous auxiliary systems uauslly needed for the ultra-precise manipulation at the microscale. We investigate the remarkable motility of the levitated droplets under different complex conditions. It is demontrated that the combination of the light-induced evaporation and the interface morphology creates ingenious vapour flow fields, as 'light-dominated vapour trap', enabling the formation of levitated droplets. The criteria for the formation and the maintenance of the levitated droplets by a single light are also elaborately discussed. Notably, the levitated droplets exhibit remarkable motility and the highly-accurate two-dimensional motility of the levitated droplets with designed velocity and trajectory above the free surface can be realized by scanning the light. This concept has significance for the development

of the light levitation technologies and in the meantime enables the highly flexible and ultra-precise manipulation of levitated femtolitre/picolitre droplets.

In this study, we use a focused light to heat a water droplet deposited on a substrate to induce the droplet evaporation accompanying with the generation of levitated droplets **(Figure 1a)**. As illustrated in **Figure 1b**, a focused laser is projected from the top to the centre of the droplet on the hydrophilic surface with a small contact angle. The droplet evaporation is immediately induced via the photothermal effect, and numerous condensed droplets are simultaneously generated above the free surface due to the localized heating source, which makes the vapour supersaturated around the interface and results in the condensation via the heterogeneous nucleation process. Because of the light-induced evaporation, the vapour flows along the interface and then vertically flows up above the original droplet centre. For the free surface with a small contact angle, the vertical flow velocity is low due to the small curvature. Such a low flow velocity enables the rapid growth of the condensed droplets, making the gravity effect non-negligible during the up-flow process. Under this circumstance, the droplets start to fall down. When the condensed droplets approach the interface, the evaporating flow from the interface carries the condensed droplets upward again, forming a vortex trajectory. This motion enables the further growth of the droplets. Once the droplet gravity is balanced with the drag force by the evaporating flow from the interface, these droplets levitate stably above the free surface. Meanwhile, the evaporation and condensation occurring at the levitated droplets are approximately in equilibrium to ensure the stabilized droplet size. Here, we examine the light-induced evaporation of a deionized water droplet (initial volume V = 4 μL) on the hydrophilic surface formed by coating polydopamine (PDA) onto the PDMS surface [32, 33], resulting in a static contact angle of ~65°. A focused laser with a wavelength of

1550 nm and a power of 200 mW is used to heat the droplet. As shown in **Figure 1c**, with the laser heating, a non-uniform temperature distribution across the droplet interface is formed. The highest interface temperature of the droplet is located at the laser point and the interface temperature is radially decreased. The condensed droplets first roll above the free surface and then levitate above the free surface around the laser beam (**Figures 1c, S1, S2a, S2b, S2e and MS1**). The volumes of the levitated droplets are ~14 pL (D: ~30 μm) at 75 s. These results suggest that the combination of the light-induced evaporation and interface-morphology creates ingenious 'light-dominated vapour trap', enabling tiny droplets to be levitated above an evaporating surface.

By contrast, in the case of the light-heated water droplet on the hydrophobic surface, it has large contact angle and curvature. The light-induced vapour flow above the free surface is more likely to rise vertically owing to the large curvature of the interface. In this case, the condensed droplets are accelerated with the upward vapour flow and acquire a relatively high velocity when they arrive at the top of the free surface. Thus, these condensed droplets are unable to stabilize above the free surface and all fly away. In this work, we also examine the light-induced evaporation of a deionized water droplet (initial volume $V = 4$ μL) on the hydrophobic surface formed by coating a thin film of polydimethylsiloxane (PDMS) onto a glass slide, resulting in a static contact angle of ~110°. As shown in **Figures S2c, S2d, S2f** and **MS2**, no levitated droplet is observed above the droplet on the hydrophobic surface although a large temperature rising is obtained. Such distinct phenomena indicate that the generation of these levitated droplets is inherently associated with the synergistic interaction between the light-induced evaporation and the vapour flow field above the free surface related to the interface morphology. It is further confirmed that the combination of an

ingenious vapour flow field arising from the interface morphology with a small curvature and the light induced evaporation is responsible for generating the levitated droplets.

We then demonstrate the proposed underlying mechanism by investigating the dynamic behaviours of the condensed droplets above the various interface morphologies via micro particle image velocimetry (μPIV, FlowMaster, LaVision, Germany). We use an aerosol generator to form dispersed aerosols above the free surface by atomizing the liquid into tiny droplets. These atomized tiny droplets afford innumerable condensation nuclei. With the growth of these tiny droplets induced by the non-equilibrium condensation/evaporation on their interface, these tiny droplets enable the generation of a large number of condensed droplets above the free surface to act as the tracer particles to simulate the condensed droplets moving trajectory. The results indicate that for the free surface with a large contact angle of ~80°, the condensed droplets are accelerated with the upward vapour flow and acquire a relatively high vertical velocity due to the large curvature of the interface. Hence, these condensed droplets keep the rising movement and all fly away (**Figure 2a** and **MS3**). By contrast, for the free surface with a small contact angle of ~20°, these condensed droplets circularly move near the light beam accompanying with the decreased vortex caused by the increased weight of the condensed droplet. Symmetrical steam swirls containing plenty of condensed droplets are created. With the growth of these condensed droplets, the final equilibrium between the droplet gravity and the drag force caused by the evaporating flow from the interface can be realized. (**Figures 2b, 2c** and **MS3**). Moreover, it is observed that the vapour flows along the interface to the localized heating source and then flows up, making the levitated droplets move to the focused laser.

We further unravel the influence of the interface morphology on the dynamics of the levitated droplets by designing the light-induced evaporation experiments with a controllable interface morphology. Here, a straight microfluidic channel with one hole at each end is fabricated by the photolithography process. First, a SU-8 (GersteltecSarl GM1075, Switzerland) film is prepared on a flat silicon wafer by spin-coating and designedly baked and exposed to the UV light. By rinsing with PGMEA (propylene glycol methyl ether acetate, Sigma-Aldrich, Germany), a mould master is fabricated on the silicon wafer. Then, the PDMS/Curing agent of 10:1 (polydimethylsiloxane, Dow Corning SYLGARD 184, United States) is poured onto the mould master and cured at 90 °C for 30 min. After peeling away, the PDMS layer is sealed with a glass slide to form the microfluidic channel. A hole with a diameter of 3.0 mm is drilled in the PDMS layer at one end of the channel as the outlet, and a hole with a diameter of 0.6 mm is drilled at the other end of the channel as the inlet. Liquid water is supplied from one end and flows out from the other end to form a water droplet. By controlling the flow rate of the supplied liquid water, the expected interface morphology of the droplet is achieved for a wide range of contact angle. A droplet with an initial contact angle of ~102° is first generated and then illuminated by a 200-mW IR laser, which causes the droplet evaporation with a decrease of the contact angle from 102° to 0°. No levitated droplet is observed at the beginning due to the large contact angle of the free surface. When the contact angle is further decreased to ~38°, the levitated droplets are rapidly generated above the free surface (**Figures 3a, 3b, 3c, S3a**). It should be mentioned that the contact angle for the appearance of the levitated droplets may slightly change due to the variation of the laser heating conditions. During the laser heating process, the maximum interface temperature of the droplet is almost unchanged, which then excludes the effect of the interface temperature (**Figures S3b, S4**). This mechanism also allows for the generation of the levitated droplets above the flat water surface and

the concave water meniscus with a small curvature (**Figures S3c, S3d**). In addition, the specific role of the laser power in the dynamics of these levitated droplets is also investigated. In the case of the hydrophobic surface, the maximum interface temperature increases to 40 °C in 54 s under a laser power of 100 mW but increases to 59 °C in 24 s under a laser power of 400 mW. The increased interface temperature results in a higher evaporation rate and thus more intense supersaturation. More condensed droplets are then generated above the free surface. However, these condensed droplets always fly away instead of levitating above the free surface; no levitated droplet is observed regardless of the laser power (**Figures 3d, 3f**). In the case of the hydrophilic surface, different results are obtained. The condensed droplets above the free surface can be formed under high laser power, and then levitate around the laser beam (**Figure 3e**). The increased laser power results in a higher evaporation rate and thus more intense supersaturation for the droplets condensation (**Figure S5**). Because the droplet on the hydrophilic surface is evaporated with the evaporation mode of the constant contact radius, the contact angle is smaller with a larger evaporation rate induced by a higher laser power. Notably, the temperature increase of approximately 20 °C relative to room temperature needed in our experiments for the occurrence of the levitated droplets is much smaller as compared to the Leidenfrost effect, which requires a critically high temperature and signifies the appearance of stable film boiling (**Figure 3g**). The variations of the interface temperature of the water droplet are analyzed. For the hydrophobic PDMS surface, as the laser heating goes on, the triple phase contact line of droplet tends to shrink after the laser-induced extension due to the hydrophobicity-dominated large receding contact angle, resulting in the evaporation mode of the constant contact angle (**Figures S2c, S2d**). With the constant contact angle mode, the temperature of the droplet is nearly maintained at high value until the end (**Figures 3f**). By contrast, for the hydrophilic PDA surface, as the laser heating goes

on, the triple phase contact line of the droplet is almost pinned at the initial position after the laser-induced extension due to the hydrophilicity-dominated low receding contact angle, resulting in the evaporation mode of the constant contact radius (**Figures S2a, S2b**). With the constant contact radius mode, the temperature of the droplet is gradually decreased because the droplet absorption length is decreased, while the heat transfer area almost remains unchanged (**Figure 3g**). Moreover, the light-induced levitated droplets can be extraordinarily stabilized above the free surface without the disappearance. Analysis of the levitated droplet size shows that the levitated droplet volume obviously changes with the laser power due to the resultant variations in the interface temperature and evaporation rate, ranging from ~33 pL (*D*: ~40 μm) to ~520 fL (*D*: ~10 μm).

One may question whether sustaining the levitated droplets requires that the two aforementioned criteria be met simultaneously. We then study the light-induced droplet evaporation while shifting the laser power from 200 mW to 100 mW. Notably, we observe an apparent difference in the requirement between generating and sustaining the levitated droplets. At low laser power, although the generation of the levitated droplets is completely suppressed as a result of the low evaporation rate, if the levitated droplets have already been generated at high laser power, some of them can still be maintained above the free surface because the evaporation is still sufficiently strong to form the evaporating flow that can sustain these levitated droplets (**Figures 4a, 4c**). But due to the change of the evaporation rate, the remained droplets undergo a new force balance between the droplets gravity and the drag force. Correspondingly, the average diameter of the levitated droplet gradually decreases from ~30 μm to ~20 μm corresponding to ~14 pL to ~4 pL droplets due to the lowered evaporation rate. We then discuss the effect of the interface morphology on the maintenance of levitated droplets by performing an experiment whereby the contact angle is

gradually increased and the laser power varies. Here, we first use a 200-mW laser to generate levitated droplets at the contact angle of ~20° and then decrease the laser power to 100 mW. As early mentioned, some levitated droplets already formed at high laser power can be sustained at 100-mW. We then increase the supply rate of the liquid water from the microfluidic channel to increase the contact angle. Interestingly, although the levitated droplets are hardly generated at large contact angles, the levitated droplets already formed at a small contact angle can still sustain even though the contact angle is larger than 80° (**Figures 4b, 4d, S6, S7**). The underlying mechanism is that with the increase of the contact angle, unlike the newly-formed tiny condensed droplets that are accelerated by the rapid vapour flow along the free surface with the large curvature and all fly away, the already-formed levitated droplets don't undergo the vertical acceleration because the drag force on the already-formed levitated droplets caused by the evaporating flow from the interface is completely counteracted by their gravity. Therefore, the already-formed levitated droplets can be maintained above the central free surface during the increase of the contact angle. Simultaneously, a new balance of the levitated droplets is formed and the average diameter increases from ~20 μm to ~40 μm corresponding to ~4 pL to ~33 pL, because of increased vertical vapour flow rate at large contact angle. These results show that the conditions required for generating levitated droplets obviously differ from those necessary for their continued existence. The generation and the maintenance of levitated droplets can be carried out as separate operations by controlling the external conditions. The achieved fundamental understanding enables us to control the quantity of the levitated droplets through the programmed switching of the laser. To this end, we first generate the levitated droplets with required quantity above the free surface at high laser power and then switch to low laser power. Thus, no new levitated droplets can be formed but the already formed levitated droplets can be sustained. As shown in **Figures 4e** and **S8**, exactly

one, two and three levitated droplets are generated. The control of the quantity of the levitated droplets allows for easily tracing individual levitated droplet.

In particular, the remarkable motility of the levitated droplets is demonstrated in this work. As described above, because the levitated droplets are always distributed around the focused laser, the movement of the levitated droplets above the free surface with remarkable flexibility and controllability can be realized by scanning the laser. We first demonstrate the movement of a levitated droplet with a specific velocity. The laser beam is precisely moved with various velocities and directions by a three-dimensional motion platform. Ultra-precise moving velocities of 50 μm/s and 200 μm/s are achieved (**Figures 5a, 5b** and **MS4)**. To quantitatively analyze the levitated droplet motility, the proportional error of the droplet moving distance, which is defined as the ratio of the difference between the droplet moving distance and the laser moving distance to the laser moving distance, is calculated. The proportional error of the droplet moving distance is less than 2.6 % with the laser moving velocity of 50 μm/s, and less than 1.4 % with the laser moving velocity of 200 μm/s, demonstrating the highly-precise motility of the light levitated droplets. Moreover, the complex movement of the levitated droplet above the free surface could be realized by moving the laser along a pre-designed route (**Figure 5c**). Furthermore, particular attention is paid to the labyrinth movement of the levitated droplet with designed trajectories above the complex grid free surface, in which several pool spots are connected by the free surface channel. As shown in **Figures 5d, 5e** and **MS5**, with the guidance of the laser, a levitated droplet is manipulated between different pool spots with a certain speed and the flexible adjustment of the moving directions. By the optional stop of the laser beam movement, the levitated droplet can be stably held at the desired position for a certain time. Thus, the light-driven arbitrary point-to-point transport of the levitated

droplets above the complex free surface can be achieved. These results fully demonstrate that a light can function as an ‘optical baton’ for the highly flexible and accurate manipulation of the levitated droplets, making this approach significantly promising for future applications of the complex materials transport and the in-situ reactions/analysis.

Furthermore, it should be pointed out that in biology and chemistry, the small amount of droplet usually contains biological or chemical components. Therefore, the creation and manipulation of the light levitated droplets with different components is important for the practical applications. In this work, we have investigated the laser-induced evaporation of the droplets containing different components rather than pure water (**Figure S9**). Experimental results indicate that 1, 2-PDO (1, 2-Propanediol 99%, Sigma-Aldrich, Germany), 1, 2-PDO/H_2O mixture (1, 2-PDO: 50%, H_2O: 50%) and 1, 2-PDO/Vegetable glycerin mixture (1, 2-PDO: 50%, Vegetable glycerin (VG): 50%, Shenzhen Daxita, China) can be used as the working fluid to generate the levitated droplets, demonstrating that the highly flexible and ultra-precise manipulation of the levitated droplets by this light method can be extended to various liquids with the appropriate properties and has significant potential in the practical applications in bioassays, pharmacy and chemosynthesis.

To summarize, we demonstrate a light method for excellently manipulating levitated liquid droplets above a free surface by a single focused laser. We confirm that the light levitation of the droplets can be achieved under mild conditions. The criteria for the formation of the levitated droplets are elaborately discussed. We demonstrate that the generation and the maintenance of levitated droplets by this light method can be carried out as separate operations by controlling the external conditions. The levitated droplets formed by this light method show extraordinary

manipulation ability. The highly-accurate two-dimensional labyrinth movement of the levitated droplets with designed trajectories above the free surface without the need for complex external architectures and surface treatment techniques is realized by scanning the light. The high-throughput, flexible and parallel manipulation of small liquid droplets can be accomplished by this concept with a well-designed light path in the future. It is believed that with the development of various designs, this promising method for generating and flexibly manipulating small levitated droplets will open new perspectives for transporting mini samples to perform reactions and analysis in biomedicine, clinical diagnosis and chemosynthesis.

Associated Content

Supporting Information Available:

Movie S1. Light levitation of droplets above the free surface.

Movie S2. Light induced evaporation of the droplet on the hydrophobic surface.

Movie S3. Droplet movement trajectory with controllable interface morphology.

Movie S4. Light manipulation of the levitated droplet movement.

Movie S5. Light-guided point-to-point movement of a levitated droplet above the grid free surface.

Figure S1. Enlarged image of the levitated droplets.

Figure S2. Laser-induced evaporation of the droplet on the hydrophilic surface and the hydrophobic surface.

Figure S3. Laser-induced evaporation with a decrease of contact angle.

Figure S4. Light-induced droplet evaporation above the free surface with different contact angles of ~20°, ~80° and ~100°.

Figure S5. Effect of the laser power on the maximum interface temperature and average evaporation rate of the water droplet.

Figure S6. Maintenance of light levitated droplets above free surface with large contact angle.

Figure S7. Light-induced droplet evaporation with an increase in the contact angle under high laser power.

Figure S8. Control of the quantity of the levitated droplets through the programmed switching of the laser.

Figure S9. The generation of the levitated droplets containing different components.

Acknowledgements

The authors gratefully acknowledge the financial supports of the National Natural Science Foundation of China (No. 51222603, No. 51576021 and No. 51620105011), the Program for Back-up Talent Development of Chongqing University (No. CQU2017HBRC1A01) and the Fundamental Research Funds for the Central Universities (No. 2018CDXYDL0001).

References

(1) Seemann, R.; Brinkmann, M.; Pfohl, T.; Herminghaus, S. Droplet Based Microfluidics. *Rep. Prog. Phys.* **2012**, *75*, 016601.

(2) Hindson, C. M.; Chevillet, J. R.; Briggs, H. A.; Gallichotte, E. N.; Ruf, I. K.; Hindson, B. J.; Vessella, R. L.; Tewari, M. Absolute Quantification by Droplet Digital PCR versus Analog Real-Time PCR. *Nat. Methods* **2013**, *10*, 1003-1005.

(3) Shim, J. U.; Ranasinghe, R. T.; Smith, C. A.; Ibrahim, S. M.; Hollfelder, F.; Huch, W. T. S.; Klenerman, D.; Abell, C. Ultrarapid Generation of Femtoliter Microfluidic Droplets for Single-Molecule-Counting Immunoassays. *ACS Nano* **2013**, *7*, 5955-5964.

(4) Culbertson, C. T.; Mickleburgh, T. G.; Stewart-James, S. A.; Sellens, K. A.; Pressnall, M. Micro Total Analysis Systems: Fundamental Advances and Biological Applications. *Anal. Chem.* **2014**, *86*, 95-118.

(5) Jebrail, M. J.; Yang, H.; Mudrik, J. M.; Lafreniere, N. M.; McRoberts, C.; Al-Dirbashi, O. Y.; Fisher, L.; Chakraborty, P.; Wheeler, A. R. A Digital Microfluidic Method for Dried Blood Spot Analysis. *Lab Chip* **2011**, *11*, 3218-3224.

(6) Onses, M. S.; Sutanto, E.; Ferreira, P. M.; Alleyne, A. G.; Rogers, J. A. Mechanisms, Capabilities, and Applications of High-Resolution Electrohydrodynamic Jet Printing. *Small* **2015**, *11*, 4237-4266.

(7) Khaw, M. K.; Ooi, C. H.; Mohd-Yasin, F.; Vadivelu, R.; St John, J.; Nguyen, N. T. Digital Microfluidics with a Magnetically Actuated Floating Liquid Marble. *Lab Chip* **2016**, *16*, 2211-2218.

(8) Zhang, Y. Z.; Zhu, B. L.; Liu, Y. H.; Wittstock, G. Hydrodynamic Dispensing and Electrical Manipulation of Attolitre Droplets. *Nat. Commun.* **2016**, *7*, 12424.

(9) Huang, N. T.; Zhang, H. L.; Chung, M. T.; Seo, J. H.; Kurabayashi, K. Recent Advancements in Optofluidics-Based Single-Cell Analysis: Optical on-Chip Cellular Manipulation, Treatment, and Property Detection. *Lab Chip* **2014**, *14*, 1230-1245.

(10) Freire, S. L. S. Perspectives on Digital Microfluidics. *Sensor. Actuat. A-Phys*. **2016**, *250*, 15-28.

(11) Samiei, E.; Luka, G. S.; Najjaran, H.; Hoorfar, M. Integration of Biosensors into Digital Microfluidics: Impact of Hydrophilic Surface of Biosensors on Droplet Manipulation. *Biosens. Bioelectron.* **2016**, *81*, 480-486.

(12) Mirica, K. A.; Ilievski, F.; Ellerbee, A. K.; Shevkoplyas, S. S.; Whitesides, G. M. Using Magnetic Levitation for Three Dimensional Self-Assembly. *Adv. Mater.* **2011**, *23*, 4134-4140.

(13) Shapiro, N. D.; Mirica, K. A.; Soh, S.; Phillips, S. T.; Taran, O.; Mace, C. R.; Shevkoplyas, S. S.; Whitesides, G. M. Measuring Binding of Protein to Gel-Bound Ligands Using Magnetic Levitation. *J. Am. Chem. Soc*. **2012**, *134*, 5637-5646.

(14) Brillo, J.; Pommrich, A. I.; Meyer, A. Relation Between Self-Siffusion and Viscosity in Dense Liquids: New Experimental Results from Electrostatic Levitation. *Phys. Rev. Lett.* **2011**, *107*, 165902.

(15) Li, J. J. Z.; Rhim, W. K.; Kim, C. P.; Samwer, K.; Johnson, W. L. Evidence for a Liquid-Liquid Phase Transition in Metallic Fluids Observed by Electrostatic Levitation. *Acta Mater.* **2011**, 59, 2166-2171.

(16) Marzo, A.; Seah, S. A.; Drinkwater, B. W.; Sahoo, D. R.; Long, B.; Subramanian,S. Holographic Acoustic Elements for Manipulation of Levitated Objects. *Nat. Commun.* **2015**, *6*, 8661.

(17) Andrade, M. A. B.; Bernassau, A. L.; Adamowski, J. C. Acoustic Levitation of a Large Solid

Sphere. *Appl. Phys. Lett.* **2016**, *109*, 044101

(18) Tseng, H.; Balaoing, L. R.; Grigoryan, B,; Raphael, R. M.; Killian, T. C.; Souza, G. R.; Grande-Allen, K. J. A Three-Dimensional Co-Culture Model of the Aortic Valve Using Magnetic Levitation. *Acta Biomater*. **2014**, *10*, 173-182.

(19) Cui, L.; Holmes, D.; Morgan, H. The Dielectrophoretic Levitation and Separation of Latex Beads in Microchips. *Electrophoresis* **2015**, *22*, 3893-3901.

(20) Abed, I.; Kacem, N.; Bouhaddi, N.; Bouazizi, M. L. Multi-Modal Vibration Energy Harvesting Approach Based on Nnonlinear Oscillator Arrays under Magnetic Levitation. *Smart Mater. Struct.* **2016**, *25*, 025018.

(21) Fedorets, A. A.; Dombrovsky, L. A.; Ryumin P. I. Expanding the Temperature Range for Generation of Droplet Clusters over the Locally Heated Water Surface. *Int. J. Heat Mass Tran.* **2017**, *113*, 1054-1058.

(22) Fedorets, A. A.; Frenkel, M.; Bormashenko, E.; Nosonovsky, M. Small Levitating Ordered Droplet Clusters: Stability, Symmetry, and Voronoi Entropy. *J. Phys. Chem. Lett*. **2017**, *8*, 5599-5602.

(23) Anyfantakis, M.; Baigl, D. Dynamic Photocontrol of the Coffee-Ring Effect with Optically Tunable Particle Stickiness. *Angew Chew*. **2015**, *126*, 14301-14305.

(24) Jiang, D.; Park, S. Y. Light-Driven 3D Droplet Manipulation on Flexible Optoelectrowetting Devices Fabricated by a Simple Spin-Coating Method. *Lab Chip* **2016**, *16*, 1831-1839.

(25) Kwon, G.; Panchanathan, D.; Mahmoudi, S. R.; Gondal, M. A.; McKinley, G. H.; Varanasi, K. K. Visible Light Guided Manipulation of Liquid Wettability on Photoresponsive Surfaces. *Nat. Commun.* **2017**, *8*, 14968.

(26) Chen, R.; Jiao, L.; Zhu, X.; Liao, Q.; Ye, D. D.; Zhang, B.; Li, W.; Lei, Y. P.; Li, D. L. Cassie-

to-Wenzel Transition of Droplet on the Superhydrophobic Surface Caused by Light Induced Evaporation. *Appl. Therm. Eng.* **2018**, *144*, 945-959.

(27) Gao, C.; Wang, L.; Lin, Y.; Li, J.; Liu, Y.; Li, X.; Feng, S.; Zheng, Y. Droplets Manipulated on Photothermal Organogel Surfaces. *Adv. Funct. Mater.* **2018**, *28*, 1803072

(28) Jiao, L.; Li, D. L; Li, W.; Chen, R.; Zhu, X.; Liao, Q.; Ye, D. D.; Zhang, B.; Wang, H. Light-Actuated Droplets Coalescence and Ion Detection on the CAHTs-Assisted Superhydrophobic Surface. *Sens. Actuators, B* **2019**, 282, 469-481.

(29) Baigl, D. Photo-Actuation of Liquids for Light-Driven Microfluidics: State of the Art and Perspectives. *Lab Chip* **2012**, *12*, 3637-3653.

(30) Zhang, T.; Chang, H. C.; Wu, Y. P.; Xiao, P. S.; Yi, N. B.; Lu, Y. H.; Ma, Y. F.; Huang, Y.; Zhao, K.; Yan X. Q. Macroscopic and Direct Light Propulsion of Bulk Graphene Material. *Nat. Photonics* **2015**, *9*, 471-476.

(31) Hassan, S. U.; Nightingale, A. M.; Niu, X. Z. Continuous Measurement of Enzymatic Kinetics in Droplet Flow for Point-of-Care Monitoring. *Analyst* **2016**, *141*, 3266-3273.

(32) Bernsmann, F.; Ponche, A.; Ringwald, C.; Hemmerle, J.; Raya, J.; Bechinger, B.; Voegel, J. C.; Schaaf, P.; Ball, V. Characterization of Dopamine-Melanin Growth on Silicon Oxide. *J. Phys. Chem. C* **2009**, *113*, 8234-8242.

(33) Liu, Y.; Ai K.; Lu, L. Polydopamine and Its Derivative Materials: Synthesis and Promising Applications in Energy, Environmental, and Biomedical Fields. *Chem. Rev.* **2014**, *114*, 5057-5115.

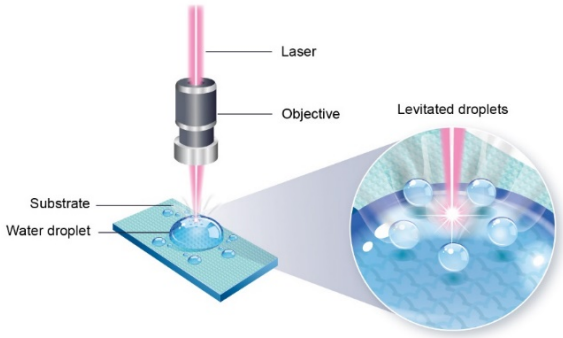

(a)

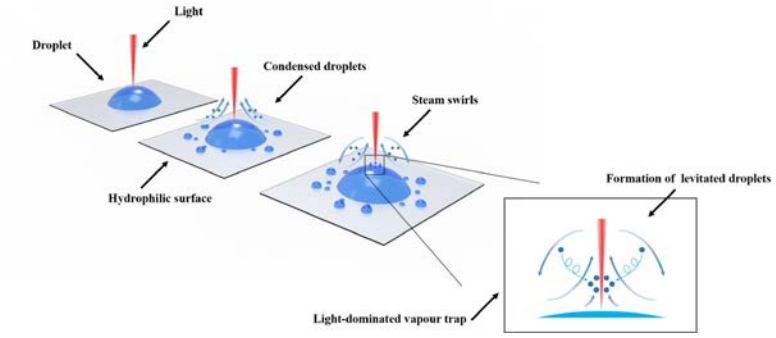

(b)

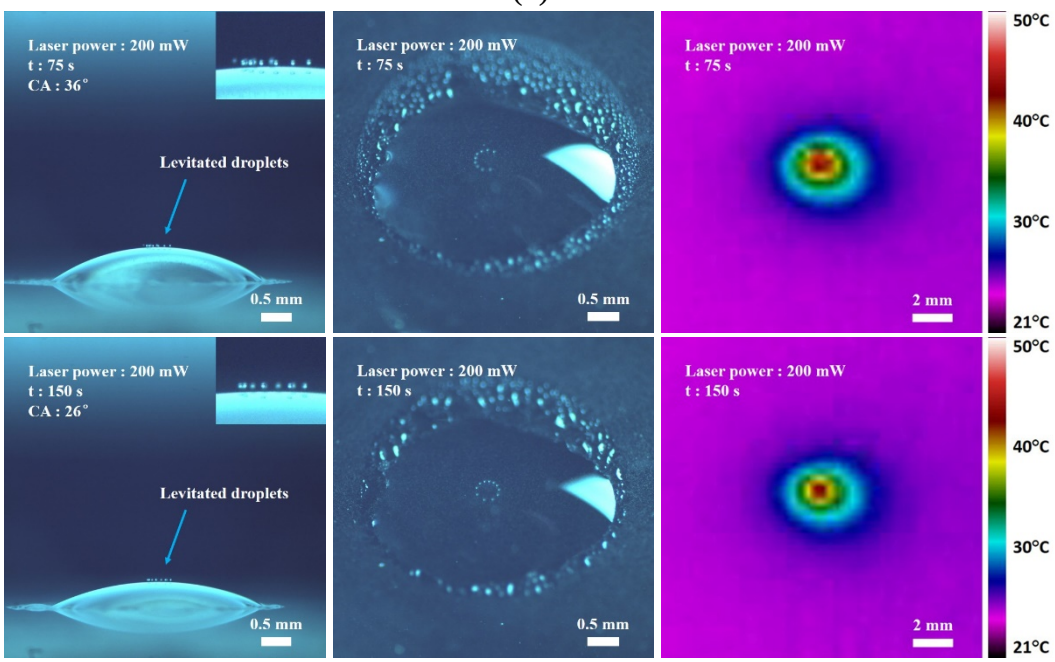

(c)

Figure 1. (a) Schematic of light-dominated vapour trap above the free surface; (b) Illustration of the evolution of condensed droplets and creation of levitated droplets; (c) Light-induced evaporation of the water droplet on a hydrophilic surface. (The magnification factor of the inserted images in Figure 1 is 2.8×.)

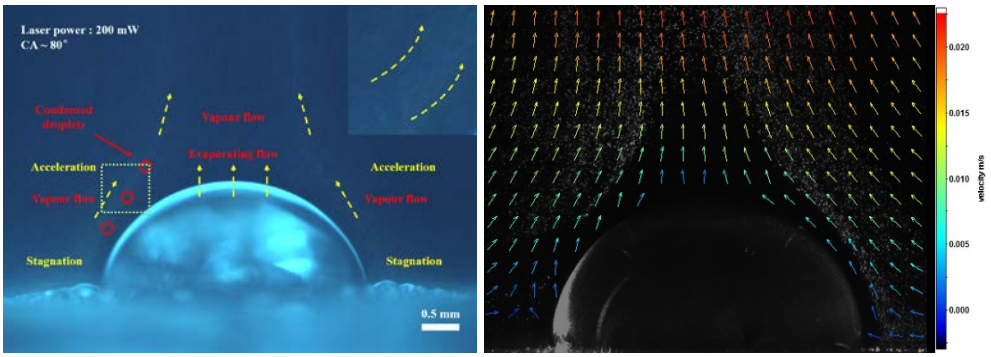

(a)

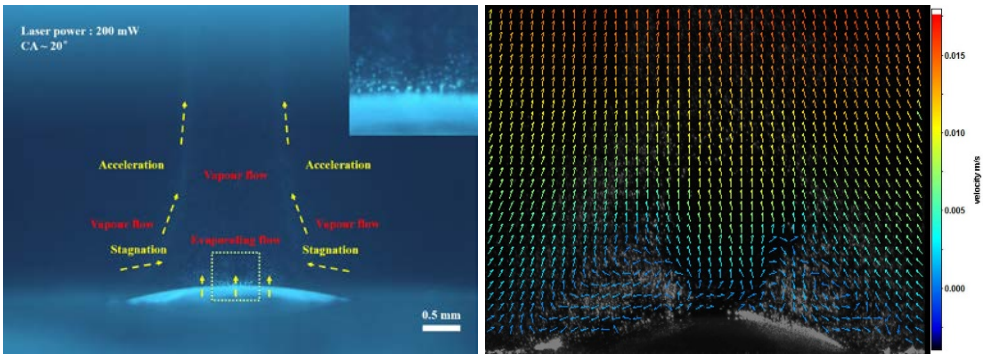

(b)

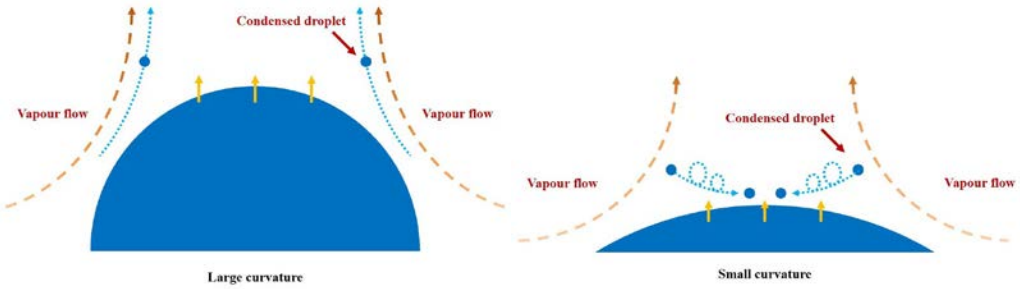

(c)

Figure 2. (a) Movement of the condensed droplets and PIV results for the velocity and moving direction of the condensed droplets above the free surface with a contact angle of ~80°; (b) Dynamic evolution process of the condensed droplets and PIV results for the velocity and moving direction of the condensed droplets above the free surface with a contact angle of ~20°; (c) Schematic illustrations of the dynamic behaviours of the condensed droplets above the free surface. (The magnification factor of the inserted images in Figure 2 is 2.8×.)

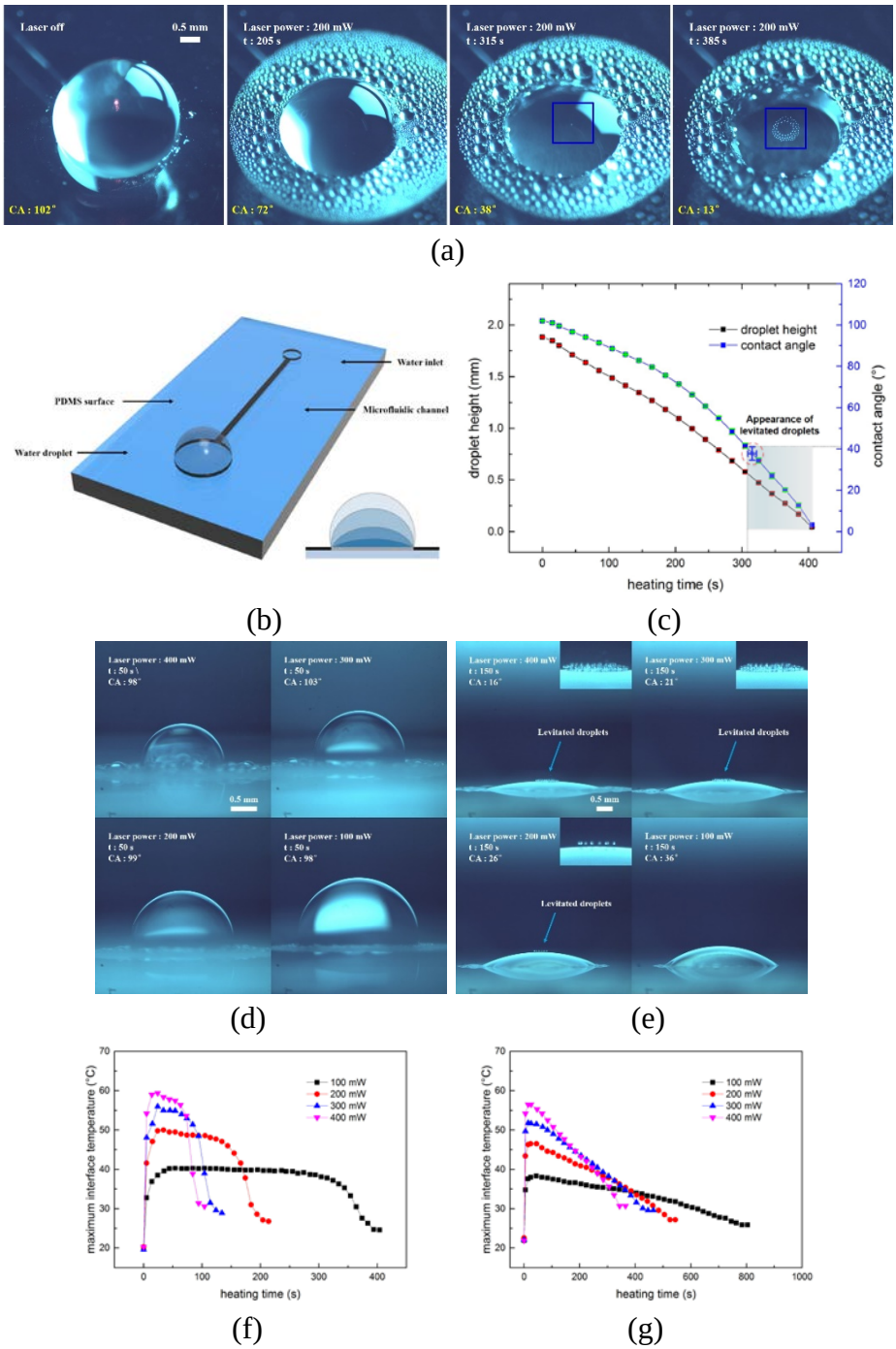

Figure 3. (a) Light-induced evaporation with a decrease of the contact angle; (b) Schematic of the microfluidic channel and evolution of the contact angle; (c) Variations of the contact angle and height of the original droplet with the laser heating process; Light-induced water droplet evaporation with different laser powers (d) on the hydrophobic surface and (e) on the hydrophilic surface; Maximum interface temperature versus the laser heating time with different laser powers (f) on the hydrophobic surface and (g) on the hydrophilic surface. (The magnification factor of the inserted images in Figure 3 is 2.8×.)

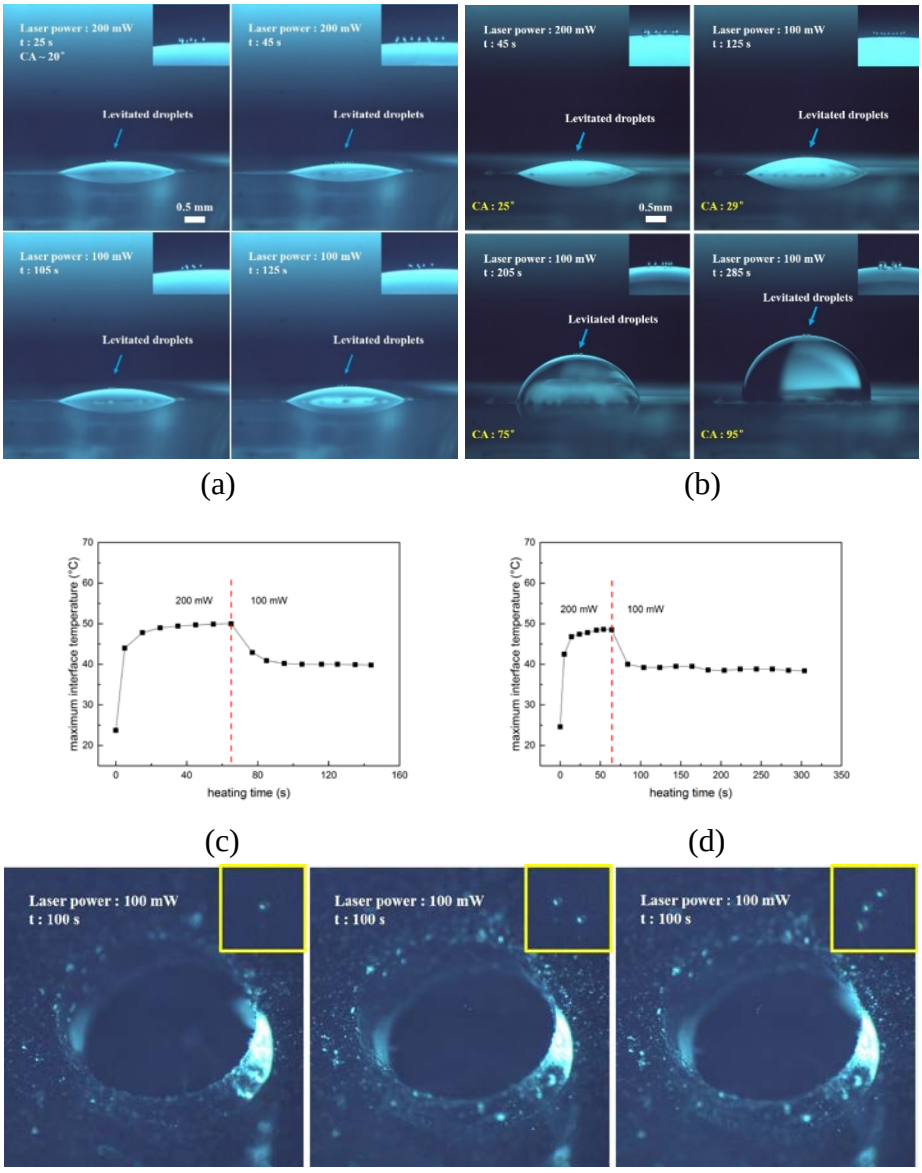

Figure 4. (a) Droplet evaporation above the free surface with a gradual decrease of laser power from 200 mW to 100 mW and maintenance of the levitated droplets above the free surface under 100 mW; (b) Light-induced levitation of droplets above the free surface with a large contact angle (Notice that the levitated droplets are first generated above the free surface with small contact angle and high laser power of 200 mW); (c) Variation of the maximum interface temperature during the laser heating process with a decrease of laser power; (d) Variations of the maximum interface temperature during the laser heating process with an increase of contact angle; (e) One, two and three levitated droplets are generated above the free surface, respectively. (The magnification factor of the inserted images is 2.8× in Figures 4a and 4b, and 5.5× in Figure 4e.)

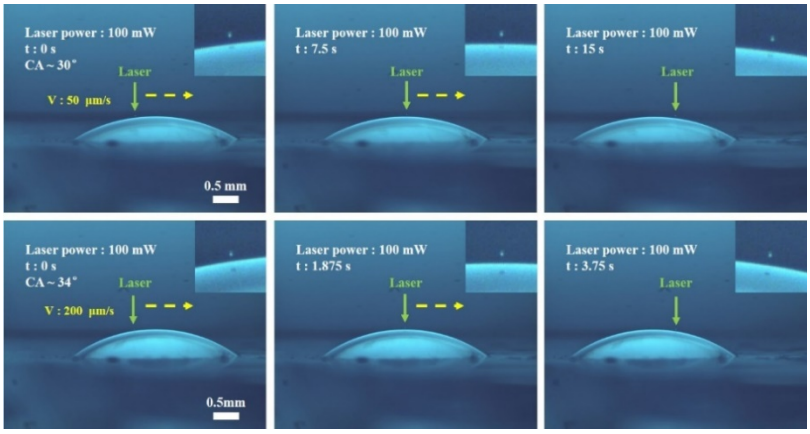

(a)

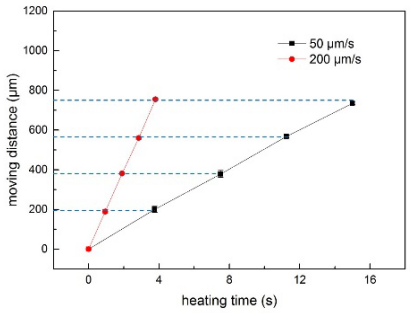

(b)

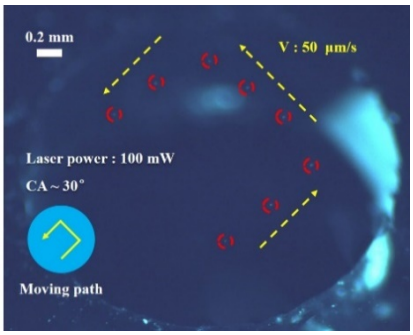

(c)

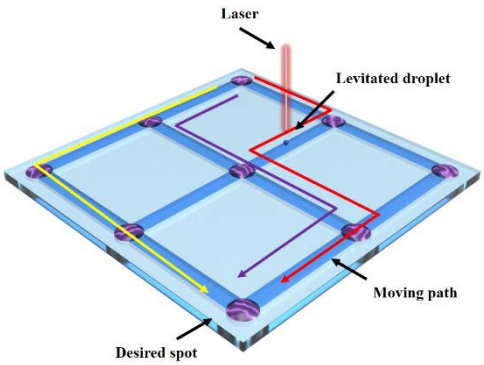

(d)

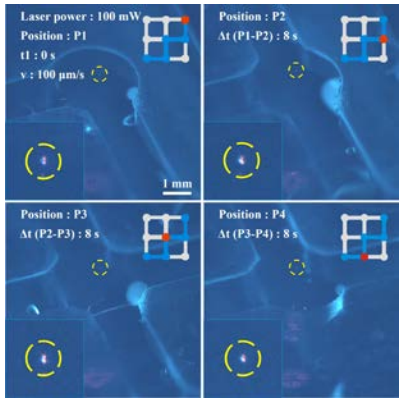

(e)

Figure 5. (a) Tunability of the moving velocities of levitated droplet; (b) Light-guided movement of a levitated droplet above the free surface with desired velocities; (c) The arbitrary movement of a levitated droplet above the free surface; (d) Schematic of the movement of levitated droplet above the grid free surface along various paths; (e) Light-guided point-to-point movement of a levitated droplet above the grid free surface. (The magnification factor of the inserted images is 5.5× in Figure 5a, and 8.2× in Figure 5e.)